



Phase transformations and mechanical properties of thermomechanically processed 34CrMo4 steel



Arun S. Thakare^{*}, S.P. Butee, R. Dhanorkar, K.R. Kambale

Department of Metallurgy and Materials Science, College of Engineering Pune, 411005, India

ARTICLE INFO

Keywords:

Materials science
Metallurgical engineering
Mechanical engineering

ABSTRACT

Precipitation hardening ferritic pearlitic (PHFP) grade 34CrMo4 steel is subjected to thermomechanical processing (TMP) for $e = 0.2$, $e = 0.4$ and $e = 0.6$ followed by furnace-, natural air- and forced air- cooling. Optical microscopy revealed the ASTM grain size number to change from 6 for the starting sample to 5–6 for the furnace cooled, 7–8 for natural air cooled and 8–9 for forced air cooled samples. A transformation from initial ferrite-pearlitic banded microstructure to almost equiaxed coarse grained ferrite-pearlitic microstructure on furnace cooling, finely distributed ferrite-bainitic microstructure on natural and forced air cooling respectively was noted. For natural and forced air cooling, the samples showed fine grained microstructure comprising of ferrite along with bainite, which became finer with increasing strain as well as cooling rate. The occurrence of ferrite-bainitic microstructures got clearly resolved in scanning electron microscopy (SEM). The microstructure of as received annealed sample in SEM revealed proeutectoid ferrite, almost linear uniformly spaced ferrite and cementite lamellae inside pearlitic nodule and uniformly distributed carbides throughout the matrix. The carbide size, otherwise remaining unchanged around 40 nm, got reduced to 23 nm only in case of forced air cooling. Extreme TMP conditions produced ferrite and broken fine colonies of bainite. The pearlite and bainite morphology assumed various forms of interlamellar spacing based on TMP. The forced air cooled ($e = 0.6$) samples demonstrated the maximum improvement in yield strength (YS = 700 MPa) by almost more than 2.5 times and in ultimate tensile strength (UTS = 790 MPa) by almost 40%. A maximum improvement in toughness (= 54 Joule) by almost 10% without loss of any other properties was observed for the TMP comprising of $e = 0.4$ and furnace cooling.

1. Introduction

In the recent past, a lot of research is focused on PHFP steels as a forging grade automotive material to attain properties comparable to, or even better than quenched and tempered (Q&T) steels by way of elimination of additional heat treatment steps involving a hardening, tempering and stress relieving cycle [1]. This is achieved by heat treatment cycle comprising of direct controlled cooling from hot forging temperature, thus saving production time as well as capacities, thereby lowering the production cost to 90% vis-à-vis Q&T steels [2, 3]. Medium carbon PHFP steels mainly find applications in automobile industry for components like diesel engine connecting rod, rotating parts of trucks, crankshaft, gear wheel and pinion shaft in place of quenched and tempered steels. This is due to their cost effectiveness and development of a ferrite-pearlitic microstructure, which imparts good toughness as well as strength achieved only by way of controlled cooling [4, 5].

PHFP steels is a group of alloy steels containing ~0.2–0.6 wt % carbon, essentially along with an addition of either of carbide forming elements like Ti, V, Nb, Cr and Mo. During their hot forging approximately at 1250 °C, vanadium and other carbides completely dissolve in austenite, forming their solid solution. A controlled cooling following this process, results in the formation of a ferrite-pearlitic microstructure along with finely dispersed precipitation of vanadium or other carbides/carbo-nitrides [6, 7]. These precipitates raise yield strength as well as the ultimate tensile strength by precipitation strengthening mechanism, which blocks the movement of dislocations to a level not far below to those observed in case of Q&T steels [3]. Further, the omission of a quenching treatment also eliminates the risk of cracking [8]. In the previous work by various researchers, the improvement of toughness is mainly attempted by controlling the microstructure through thermo-mechanical processing. A variety of microstructures i.e. acicular ferrite, grain boundary ferrite, pearlite,

^{*} Corresponding author.

E-mail address: arun.thakare@gmail.com (A.S. Thakare).

<https://doi.org/10.1016/j.heliyon.2019.e01610>

Received 3 December 2018; Received in revised form 25 January 2019; Accepted 26 April 2019

2405-8440/© 2019 Published by Elsevier Ltd. This is an open access article under the CC BY-NC-ND license (<http://creativecommons.org/licenses/by-nc-nd/4.0/>).

bainite and martensite were obtained by them depending upon the deformation temperatures and cooling rates used [9, 10, 11]. Bleck et al. obtained good toughness while maintaining high strength values with development of ferrite-pearlitic and bainitic microstructures [12]. Nurnberger et al. studied the microstructure transformations in 34CrMo4 during continuous cooling from hot forging temperatures and found that with the rise in cooling rate from 0.04 Ks^{-1} to 30 Ks^{-1} , microstructure changed from ferrite-pearlite to bainite and further to martensite on additional increase in cooling rate. Accordingly, an increase in hardness from 165 HV to 301 HV and further to 556 HV was noted [4]; no other mechanical properties were reported by these authors. They also studied the effect of deformation percentage on martensite start (Ms) temperature. The Ms temperature showed an increase as deformation percentage increased; whereas, the pearlite start temperature was not affected much. For comparison sake, it would be appropriate to mention here the properties of the quenched and tempered 34CrMo4 steel currently being used in industry. These are $YS = 703 \text{ MPa}$, $UTS = 814 \text{ MPa}$, hardness = 245 BHN and % elongation = 22 [13].

Other medium carbon PHFP steels viz 30MsV6, S43C, 38MnSiV5, 42CrMo4 etc. were also studied for different deformation temperatures, deformation percentages and cooling conditions. Rasouli et al. studied the effect of deformation temperature and cooling rate on 30MsV6 and observed that the UTS increased from 860 MPa to 1183 MPa and hardness from 245 HV to 322 HV at $850 \text{ }^\circ\text{C}$ deformation temperature. This was attributed to formation of acicular ferrite and pearlite [7]. For the same steel, as the cooling rate was increased from $3 \text{ }^\circ\text{C/s}$ to $15 \text{ }^\circ\text{C/s}$, phases changed from acicular ferrite and pearlite to bainite and finally to martensite, and the UTS increased from 860 MPa to 1535 MPa and hardness increased from 245 HV to 542 HV [8]. Hara et al. studied the effect of finish forging temperature ($950 \text{ }^\circ\text{C}$ – $1120 \text{ }^\circ\text{C}$) on S43C steel. They observed that the forging done at $1050 \text{ }^\circ\text{C}$ resulted into good combination of UTS of 950 MPa and toughness of 28 Joule. This was attributed to limited dissolution of carbides in austenite at this temperature [14]. Dini et al studied the effect of cooling rate and preheating temperature on 38MnSiV5 steel. Therein, as the cooling rate increased from still air – to forced air – to water cooling, the UTS increased from 870 to 950 and finally to 1100 MPa, that too without much effect on toughness values. This was attributed to restricted growth of austenite grains and increased driving force for reprecipitations of dissolved carbonitrides during water cooling after hot forging, which contributed to increased nucleation sites for precipitation and production of finer carbonitrides [15, 16, 17]. A preheating temperature of $1100 \text{ }^\circ\text{C}$ also gave good combination of mechanical properties i.e. UTS = 880 MPa and toughness = 18 Joule. However, as the preheating temperature was increased beyond $1100 \text{ }^\circ\text{C}$, all the carbides got dissolved in austenite and precipitated out as impurity particles. Even though these contributed to an increase in strength, the toughness was reduced. For a preheating temperature less than $1100 \text{ }^\circ\text{C}$, limited dissolution of carbides in austenite occurred, which contributed to a marginal decrease in UTS to 850 MPa and a small increase in toughness to 19 Joule [15].

A critical evaluation of all the above mentioned literature, there is hardly any evidence of detailed microstructure investigation by SEM and its correlation to the mechanical properties. Many have reported changes in hardness only, whereas, others have reported toughness and strength without detailed investigation of microstructures. No clear evidence of occurrence of pearlite or bainite phase is available as their clear distinction with optical microscopy becomes difficult. The evidence of carbide precipitation also appears incomplete with lack of supporting microstructures. Further, the contribution coming from grain refinement is also not discussed in details. Improvement in toughness values is one of the important aspects in development of these steels for their life improvement and wider areas of applications. The present investigation attempts to address all the above issues of concern in development of

PHFP steels.

2. Experimental

The material used for this research work was medium carbon microalloy steel 34CrMo4. Chemical composition of 34CrMo4 is given in Table 1.

Round steel bar with 40 mm diameter were reheated at $1100 \text{ }^\circ\text{C}$ for 60 min. and forged at $1050 \text{ }^\circ\text{C}$ for $e = 0.2$, $e = 0.4$ and $e = 0.6$. After deformation samples were given three different types of cooling i.e. furnace-, natural air- and forced air-cooling. Thermomechanical processing sequence employed is given in Fig. 1.

The nomenclature used for identification of samples is given in Table 2.

The vickers hardness tester (Make-FIE/Model no TV- 50) was used to determine vickers hardness number (VHN/HV) as per ASTM E10 standard. Tensile test was carried out on tension-compression (Universal motion/TUE-CN-600) testing machine. Round specimens as per ASTM A 370 standard was used and strain rate $0.5 \text{ } (\% \text{ strain/min})$ and load rate 10 kN/min was used for tensile test as strain rate increased stresses are also increased and affect the tensile properties. The extensometer was removed after yielding and loading was continued until failure. The impact toughness test was conducted on Pendulum impact machine with impact energy capacity 300 Joule max. (Make FIE, Model IT – 30). A standard specimen as per ASTM E23 was used for conducting the Charpy impact test.

Microstructures were observed at 100X–500X magnifications under Optical Microscope (Conation, suXma-Met-1). 4% nital was used as etchant. Compositions of phases (size and amount) present were analyzed using Image analyzer software (make Conation Technology). SEM images were taken for 10KX and 50KX magnification on SEM-EDS (Carl Zeiss, SIGMA HV-BRUKER) with acceleration voltage of 15 KV.

3. Results and discussion

Metallurgically, the contribution to strengthening is expected to come from strain hardening (includes phase transformation), precipitation hardening, solid solution strengthening and grain refinement [18]. Hence it is attempted herewith to understand and correlate the effect of all these factors on the achieved properties as discussed below.

3.1. Optical microscopy of 34CrMo4 steel

Microstructure of 34CrMo4 before ($e = 0.0$) and after thermo-mechanical processing at $1050 \text{ }^\circ\text{C}$ for $e = 0.2$, $e = 0.4$ and $e = 0.6$ and cooling with three different rate i.e. furnace-, natural air- and forced air cooling are shown in Fig. 2. It is observed that the microstructure of the starting annealed 34CrMo4 steel viz. $A_S (0.0)$ shows a banded microstructure comprising of coarse grains of ferrite and pearlite. As expected, this microstructure transforms into an equiaxed grained ferrite-bainitic microstructure with the increase in cooling rate to natural and forced air cooling ($A_N (0.0)$ and $A_F (0.0)$ samples), the grains becoming finer for forced air cooling ($A_F (0.0)$). No deformation being applied here for all these three samples ($A_S (0.0)$, $A_N (0.0)$ and $A_F (0.0)$). After heating this steel to $1100 \text{ }^\circ\text{C}$, subsequent hot deformation at $1050 \text{ }^\circ\text{C}$ and controlled cooling, the austenite gets transformed into ferrite, pearlite and bainite depending on the strain induced during thermomechanical processing and the cooling rate incorporated. The furnace cooled samples $A_S (0.2)$, $A_S (0.4)$ and $A_S (0.6)$ shows coarse grain boundary ferrite and pearlite [11]. These microstructures show large size grain than as received samples due to recovery, recrystallisation and grain growth taking place during furnace cooling, which outcaste the effect of prior strain. However, the grains appear to become more equiaxed at higher strains rate samples i.e. $e = 0.4$ and $e = 0.6$. The natural air cooled samples $A_N (0.2)$, $A_N (0.4)$, and $A_N (0.6)$ shows a fine grained microstructure mainly comprising of ferrite along with fewer content of bainite. The amount of bainite is noted to increase in case of the forced air cooled samples A_F

Table 1
Chemical composition.

Grade	C	Mn	Si	S	P	Cr	Mo	V/Nb
34CrMo4 (Std specified range)	0.30–0.37	0.50–0.80	0.15–0.40	0.035 max	0.035 max	0.90–1.20	0.15–0.30	
34CrMo4 (Actual)	0.30	0.56	0.25	0.020	0.017	1.00	0.17	0.001

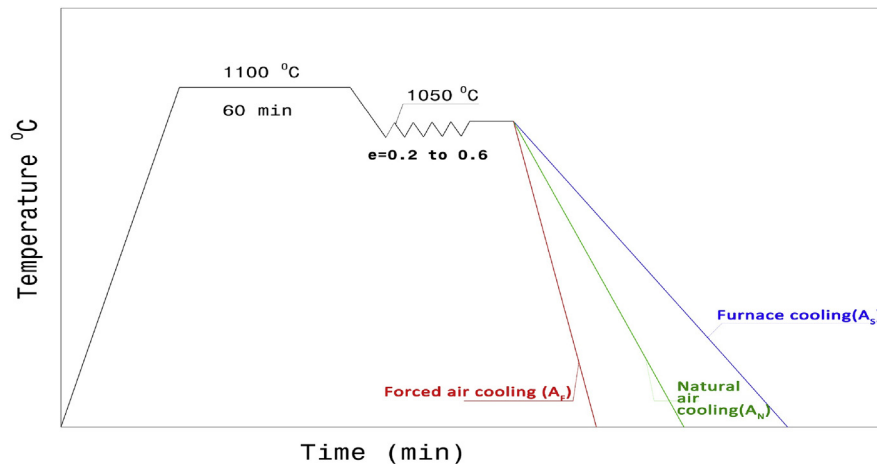


Fig. 1. Thermal cycles used for TMP of 34CrMo4 steel showing forced air cooling (A_F), natural air cooling (A_N) and furnace cooling (A_S).

Table 2
Nomenclature of samples.

Sr. no.	Method of cooling	Strain	Nomenclature
1	Furnace cooling	$e = 0.0$	$A_S (0.0)$
2	Furnace cooling	$e = 0.2$	$A_S (0.2)$
3	Furnace cooling	$e = 0.4$	$A_S (0.4)$
4	Furnace cooling	$e = 0.6$	$A_S (0.6)$
5	Natural air cooling	$e = 0.0$	$A_N (0.0)$
6	Natural air cooling	$e = 0.2$	$A_N (0.2)$
7	Natural air cooling	$e = 0.4$	$A_N (0.4)$
8	Natural air cooling	$e = 0.6$	$A_N (0.6)$
9	Forced air cooling	$e = 0.0$	$A_F (0.0)$
10	Forced air cooling	$e = 0.2$	$A_F (0.2)$
11	Forced air cooling	$e = 0.4$	$A_F (0.4)$
12	Forced air cooling	$e = 0.6$	$A_F (0.6)$

(0.2), $A_F (0.4)$ and $A_F (0.6)$, again showing the same phases, however these appear in form of distorted colonies here. The CCT diagram for 34CrMo4 steel [4] shows a clearly separated bainite region, which lies towards the left side of the pearlitic nose in the diagram. Because of faster cooling, the cooling rate escapes the nose of CCT diagram, enter into bainitic bay and transform to bainite. In case of the natural air cooled ($A_N (0.2)$ to $A_N (0.6)$) and forced air cooled ($A_F (0.2)$ to $A_F (0.6)$) samples, for the same cooling rate, as the strain increases, the grain size decreases. All these aspects are more elaborately discussed in section 3.3 on SEM analysis.

3.2. Grain and precipitate size determination

Table 3 shows the ASTM grain number and precipitate size (mostly carbides) of samples deformed at $e = 0$, $e = 0.2$, $e = 0.4$ and $e = 0.6$ with furnace-, natural air- and forced air cooling. For the as received ($e = 0$) samples grain size was noted to be between 6 and 7. On subsequent processing, the effect of cooling rate demonstrated an increase in grain size for the furnace cooled samples, with the ASTM grain size number (n) marginally reducing to $n = 5$ –6 for $e = 0.4$, whereas, it demonstrated a value of $n = 5$ for the other two deformations ($e = 0.2$ and $e = 0.6$). This got reflected in a balance of high toughness and high strength values

noted for these ($A_S (0.4)$) samples (see Fig. 4). While cooling with natural air and forced air, the grain size was reduced to 7–8 and 8–9 respectively due to combined effect of plastic deformation associated with TMP and faster cooling rates, which prevented the growth of austenite grains. This grain refinement positively contributed to an associated increase in strength, without corresponding improvement in toughness (see Fig. 4), may be because of more distortions of bainite for higher deformations (see Fig. 3 for $A_N (0.2)$ – $A_N (0.6)$ and $A_F (0.2)$ – $A_F (0.6)$ samples). While noting the effect of deformation, the extent of grain refinement was: for $e = 0.6$ ($n = 8$ –9) > $e = 0.4$ ($n \sim 8$) > $e = 0.2$ ($n = 7$ –8), except for furnace cooling for all deformations.

In case of the size of the precipitates obtained on TMP, only faster cooling for the as received samples reduced the precipitate size from 40 to 23 nm. For all the other TMP conditions the precipitate size remains between 38 to 48 nm (10 nm size difference). This has contributed marginally to the changes in properties noted apart from other factors involved [19, 20, 21].

3.3. SEM analysis of 34CrMo4 steel

SEM images of the TMP samples recorded at 50KX magnification are shown in Fig. 3. The inset shows SEM images of the same samples taken at 10KX. In the as received annealed sample $A_S (0.0)$, a ferrite-pearlitic microstructure is seen. The presence of a ferrite-bainitic microstructure for $A_N (0.0)$ and $A_F (0.0)$ samples got confirmed in SEM. The furnace cooled samples $A_S (0.2)$ – $A_S (0.6)$ shows the presence of ferrite and pearlite, in agreement with optical microscopy. The interlamellar spacing of pearlite goes on decreasing with increase in strain. The natural air cooled samples $A_N (0.2)$ – $A_N (0.6)$ and the forced air cooled $A_F (0.2)$ – $A_F (0.6)$ samples show presence of ferrite and bainite only. The increase of strain as well as cooling rate further caused the bainite to become finer and distorted. The CCT diagram also reveals occurrence of ferrite and pearlite or bainite in different temperature ranges for 34CrMo4 steel [4].

Apart from this, the undissolved carbides together with hot deformation are likely to cause inhomogeneous distribution of carbon in prior deformed austenite [22]. These inhomogeneities are likely to provide increased number of nucleation site for bainite, thereby forming more

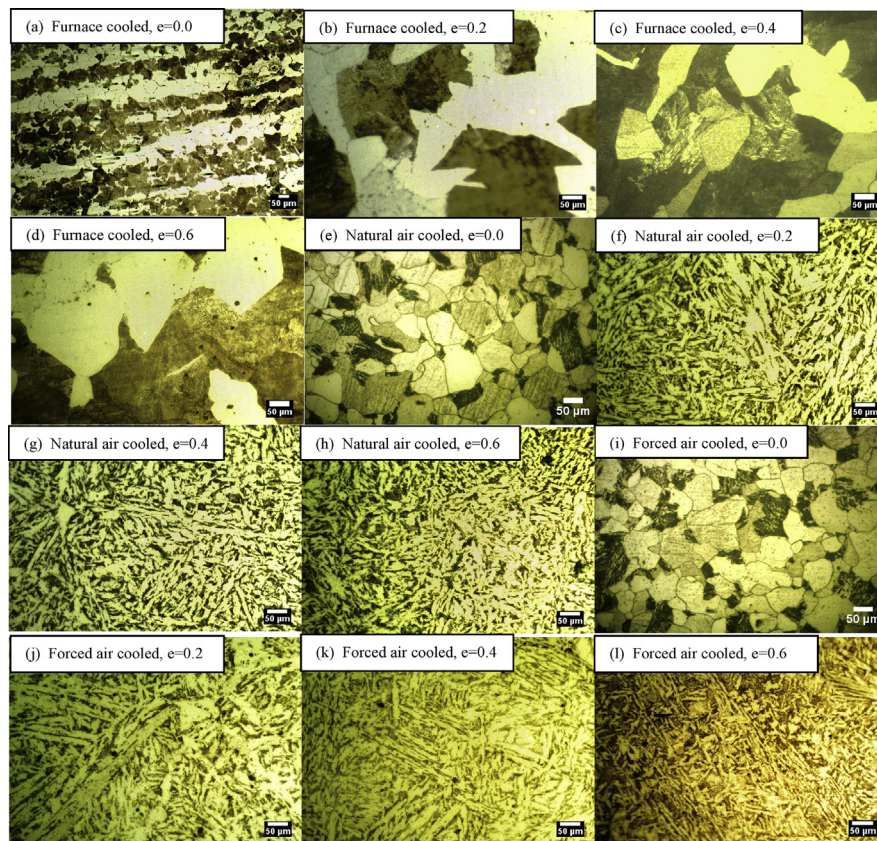


Fig. 2. Microstructures of TMP specimen; Furnace cooled (a) strain, $e = 0.0$, nomenclature is $A_S (0.0)$, (b) $A_S (0.2)$, (c) $A_S (0.4)$, (d) $A_S (0.6)$, Natural air cooled (e) $A_N (0.0)$, (f) $A_N (0.2)$, (g) $A_N (0.4)$, (h) $A_N (0.6)$. Forced air cooled (i) $A_F (0.0)$, (j) $A_F (0.2)$, (k) $A_F (0.4)$, (l) $A_F (0.6)$.

Table 3

ASTM grain size number and precipitate size of all TMP samples.

Specimen nomenclature	ASTM grain size no. (It is inversely related to actual grain size)	Average precipitate size (in nm measured at 100 KX)
$A_S (0.0)$	6	40
$A_S (0.2)$	5	48
$A_S (0.4)$	5–6	39
$A_S (0.6)$	5	44
$A_N (0.0)$	6–7	30
$A_N (0.2)$	7–8	41
$A_N (0.4)$	8	44
$A_N (0.6)$	8–9	38
$A_F (0.0)$	7	23
$A_F (0.2)$	8	46
$A_F (0.4)$	8–9	42
$A_F (0.6)$	8	42

number of bainite colonies and their reduced size. No apparent change in the form of proeutectoid ferrite is noted with change of cooling and strain rate. The carbides are also noted to become finer and more distributed with increasing strain and cooling rate, which is also likely to improve the strength and reduce the impact toughness.

It was also attempted to know the dissolution of carbides in austenite matrix on heating the samples between 1050, 1150 and 1250 °C followed by water quenching [6]. Our presumption was that the carbides (size and content) would reduce on heating the samples at higher temperatures and there will be no carbides seen at 1250 °C. Even though the observed carbide content was less, it could not be established whether these carbides got reprecipitated out on quenching or some remained undissolved at 1250 °C.

3.4. Mechanical properties of as received material and after hot deformation (Thermomechanical process)

The effect of strain and the cooling rate on mechanical properties is shown in Fig. 4. The values for the annealed $A_S (0.0)$ sample are taken as base line for comparison of properties. A monotonic marginal gain in toughness values is observed for the furnace cooled $A_S (0.2)$ & $A_S (0.4)$ samples. Only a marginal drop in toughness accompanied by a rise in strength parameters for the furnace cooled $A_S (0.6)$ sample (at $e = 0.6$ strain) is noted. Even though the application of strain caused reduction in toughness and improvement in strength, the same trend of marginal reduction in toughness and marginal improvement in strength with increase in strain from $e = 0.2$ to 0.6 is noted for natural ($A_N (0.2) - A_N (0.6)$) and forced air ($A_F (0.2) - A_F (0.6)$) cooling conditions introduced. The highest improvement in toughness by almost 10% without loss of any other properties is observed for $A_S (0.4)$ samples. This is attributed to a coarse equiaxed grain microstructure comprising of ferrite and pearlite. As expected, for the forced air cooled sample with $e = 0.6$, the maximum improvement in YS by almost more than 2.5 times and in UTS by almost 40% with some loss of toughness and elongation is noted. In case of all the TMP samples processed, it is noted that there is an improvement in YS, UTS and hardness at the expense of some loss of toughness and elongation values. This is attributed to a two phase microstructure of fine ferrite and bainite, both becoming still finer with increasing strain and cooling rate, apart from unrecovered residual stresses introduced during TMP followed by fast cooling. Looking at the overall values of the properties, it appears that the cooling rate plays a more dominant effect than the strains incorporated. In general, all the above changes noted in mechanical properties are attributed to an almost equiaxed grain microstructure for the furnace cooled samples and a fine bainitic microstructure for both natural and forced air cooled samples, the bainite showing more distortion in case of forced air cooling ($A_F (0.2) - A_F (0.6)$).

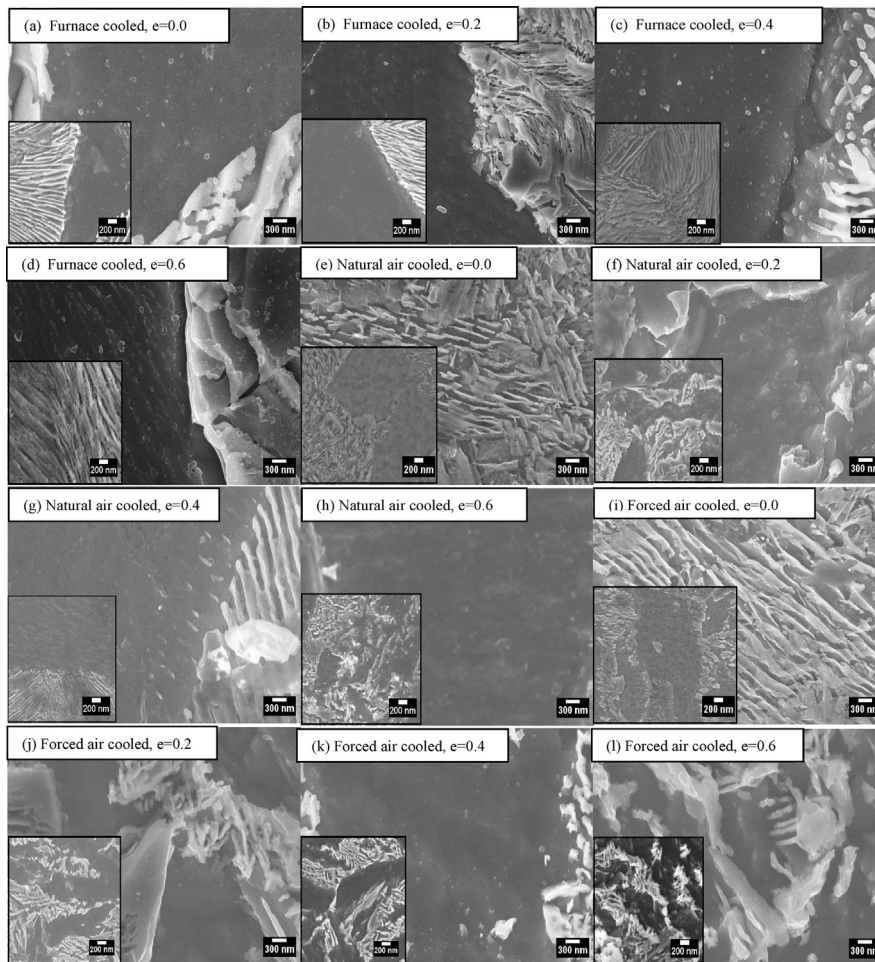


Fig. 3. SEM image of TMP specimen (The inset shows a lower magnification view for each of the TMP employed); Furnace cooled (a) strain, $e = 0.0$, nomenclature is $A_S(0.0)$, (b) $A_S(0.2)$, (c) $A_S(0.4)$, (d) $A_S(0.6)$, Natural air cooled (e) $A_N(0.0)$, (f) $A_N(0.2)$, (g) $A_N(0.4)$, (h) $A_N(0.6)$. Forced air cooled (i) $A_F(0.0)$, (j) $A_F(0.2)$, (k) $A_F(0.4)$, (l) $A_F(0.6)$.

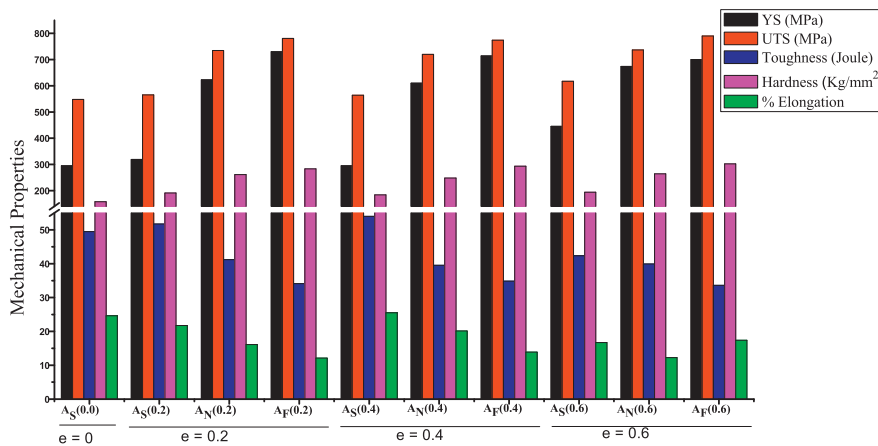


Fig. 4. Column chart showing variation of the mechanical properties (YS, UTS, impact toughness, hardness and % elongation) with TMP for 34CrMo4 steel specimens.

The mechanical properties demonstrated a good correlation to the observed microstructures. Overall the occurrence of bainite has caused improvement in strength without much loss of toughness.

4. Conclusions

Both optical microscopy and SEM revealed the presence of coarse

ferrite-pearlitic polygonal grains only in case of furnace cooled samples and a ferrite-bainitic microstructure for all the natural and forced air cooled samples. The ferrite-bainitic microstructures became finer and more distorted with increase of both cooling rate and strain. An improvement in toughness (= 54 Joule) by almost 10% without loss of any other properties was observed for $e = 0.4$ and furnace cooling. As expected the forced air cooled samples demonstrated the maximum

improvement in YS (= 700 MPa) by almost more than 2.5 times and in UTS (= 790 MPa) by almost 40% with some loss of toughness and elongation. These values were obtained spending much less time and energy vis-à-vis quench and tempered steels. A good balance of UTS (= 720 MPa), %E (= 20 %) and toughness (= 40 Joule) was noted for e = 0.4 and natural air cooled samples.

Declarations

Author contribution statement

Arun S. Thakare, S. P. Butee: Conceived and designed the experiments; Performed the experiments; Analyzed and interpreted the data; Contributed reagents, materials, analysis tools or data; Wrote the paper.

R. Dhanorkar: Performed the experiments.

K. R. Kambale: Contributed reagents, materials, analysis tools or data.

Funding statement

This research did not receive any specific grant from funding agencies in the public, commercial, or not-for-profit sectors.

Competing interest statement

The authors declare no conflict of interest.

Additional information

No additional information is available for this paper.

References

- [1] C. Keul, V. Wirth, W. Blek, New bainitic steel for forging, *Arch. Civil Mech. Eng.* 12 (2012) 119–125.
- [2] S. Sankaran, V. Subramanya Sarma, V. Kaushik, K.A. Padmanabham, Thermo mechanical processing and characterization of multi phase microstructure in V-bearing medium carbon micro-alloyed steel, *J. Mater. Process. Technol.* 139 (2003) 642–647.
- [3] Gernot, Buchmayr Bruno, *High Strength Bainitic Steels for Forged Products*, Springer-Verlag Wien, BHM, 2015, pp. 1–5.
- [4] F. Nurnberger, O. Grydin, M. Schaper, F.W. Bach, B. Koczurkiewicz, A. Milenin, Microstructure transformations in tempering steels during continuous cooling from hot forging temperatures, *Steel Res. Int.* 81 (No. 3) (2010) 224–233.
- [5] R.M.K. Honeycombe, H.K.D.H. Bhadeshia, *Steels, Microstructure and Properties*, third ed., 42, Arnold, London, 2006, pp. 142–155.
- [6] Monideepa Mukherjee, Ulrich Prael, Wolfgang Bleck, Modelling the strain-induced precipitation kinetics of vanadium carbonitride during hot working of precipitation-hardened Ferritic–Pearlitic steels, *Acta Mater.* 71 (2014) 234–254.
- [7] Xiangwei Kong, Liangyun Lan, Zhiyong Hu, Bin Li, Tianzhong Sui, Optimization of mechanical properties of high strength bainitic steel using thermo-mechanical control and accelerated cooling process, *J. Mater. Process. Technol.* 217 (2015) 202–210.
- [8] Ing Hans Willi Raedt, Ulrich Speckenheuer, Dipl.-Ing Klaus Vollrath, New forged steels energy efficient solutions for stronger parts, *ATZ Autotechnol.* 12 (2012) 13–17.
- [9] D. Rasouli, Sh. Khameneh Asl, A. Akbarzadeh, G.H. Daneshi, Optimization of mechanical properties of a micro-alloyed steel, *Mater. Des.* 30 (2009) 2167–2172.
- [10] D. Rasouli, Sh. Khameneh Asl, A. Akbarzadeh, G.H. Daneshi, Effect of cooling rate on the microstructure and mechanical properties of micro-alloyed forging steel, *J. Mater. Process. Technol.* 206 (2008) 92–98.
- [11] Piotr Skubisz, Łukasz Lisiecki, Piotr Micek, Effect of direct cooling conditions on characteristics of drop forged Ti+V+B microalloy steel, *Proc. Manuf.* 2 (2015) 428–433.
- [12] W. Bleck, et al., *Advances in Production Technology, Lecture Notes in Production Engineering*, Christian Brecher Editor, 2013, pp. 88–94.
- [13] V.B. Bhandari, *Machine Design Data Book*, McGraw Hill Education (India) Private Limited, 2014, 2.16.
- [14] H. Hara, M. Kobayashi, The Use of Hot Forged Micro-alloyed Steel in Automobile Components, Institute of Metals Vanadium Award Paper, 1987, pp. 5–15.
- [15] Ghasem Dini, Mahmood Monir Vaghefi, Shafeyi Ali, The influence of reheating and direct cooling rate after forging on microstructure and mechanical properties of V-microalloyed steel 38MnSiV5S5, *ISIJ Int.* 46 (1) (2006) 89–92.
- [16] K.A. Padmanabhan, S. Sankaran, Fatigue behavior of a multiphase medium carbon V-bearing micro-alloyed steel processed through two thermo mechanical routes, *J. Mater. Process. Technol.* 207 (2008) 293–300.
- [17] V.V. Natrajan, V.S.A. Challa, R.D.K. Misra, D.M. Sidorenko, M.D. Mulholland, M. Manohar, J.E. Hartmann, The determining impact of cooling temperature on the microstructure and mechanical properties of a Titanium-Niobium ultrahigh strength microalloyed steel, *Mater. Sci. Eng.* 665 (2016) 1–9.
- [18] F. Nurnberger, O. Grydin, Z. Yu, M. Schaper, Microstructural behavior of tempering steels during precision forging and quenching from hot-forming temperatures, *Metall. Min. Ind.* 3 (7) (2011) 79–86.
- [19] Gaung Xu, Xiaolong Gan, Guojun Ma, Feng Luo, Hang Zou, The development of Ti-alloyed high strength microalloy steel, *Mater. Des.* 31 (2010) 2891–2896.
- [20] H. Jirkova, L. Kudrova, B. Masek, The effect of chromium on microstructure development during Q-P Process, *Mater. Today Process.* 2S (2015) S627–S630.
- [21] S. Gunduza, R.C. Cochrane, Influence of cooling rate and tempering on precipitation and hardness of vanadium microalloyed steel, *Mater. Des.* 26 (2005) 486–492.
- [22] L.M. Kaputkina, D.E. Kaputkin, Structure and phase transformation under quenching and tempering during heat and thermomechanical treatment of steel, *Mater. Sci. Forum* 426–432 (2003) 1119–1126.